Published in final edited form as:

Cancer Res. 2021 May 01; 81(9): 2373–2385. doi:10.1158/0008-5472.CAN-20-3222.

Platelet TLR4-ERK5 axis facilitates NET-mediated capturing of circulating tumor cells and distant metastasis after surgical stress

Jinghua Ren[1,2,3,†], **Jiayi He**[1,4,†], **Hongji Zhang**[1,5], **Yujia Xia**[1,6], **Zhiwei Hu**[1], **Patricia Loughran**[3,7], **Timothy Billiar**[3], **Hai Huang**[1,§], **Allan Tsung**[1,§]

[1]Department of Surgery, The Ohio State University Medical Center, Columbus, Ohio 43210, USA

[2]Cancer center, Union Hospital, Huazhong University of Science and Technology, Wuhan 430022, P.R. China

[3]Department of Surgery, University of Pittsburgh Medical Center, Pittsburgh, Pennsylvania 15213, USA

[4]Department of Pediatrics, Tongji Hospital, Huazhong University of Science and Technology, Wuhan 430030, P.R. China

[5]Department of Surgery, Union Hospital, Huazhong University of Science and Technology, Wuhan 430022, P.R. China

[6]Department of Gastroenterology, Tongji Hospital, Huazhong University of Science and Technology, Wuhan 430030, P.R. China

[7]Center for Biologic Imaging, Department of Cell Biology, University of Pittsburgh Medical Center, Pittsburgh, Pennsylvania 15213, USA

Abstract

Surgical removal of malignant tumors is a mainstay in controlling most solid cancers. However, surgical insult also increases the risk of tumor recurrence and metastasis. Tissue trauma activates the innate immune system locally and systemically, mounting an inflammatory response. Platelets and neutrophils are two crucial players in the early innate immune response that heals tissues, but their actions may also contribute to cancer cell dissemination and distant metastasis. Here we report that surgical stress-activated platelets enhance the formation of platelet-tumor cell aggregates, facilitating their entrapment by neutrophil extracellular traps (NET) and subsequent distant metastasis. A murine hepatic ischemia/reperfusion (I/R) injury model of localized surgical stress showed that I/R promotes capturing of aggregated circulating tumor cells (CTC) by NETs and eventual metastasis to the lungs, which are abrogated when platelets are depleted. Hepatic I/R also increased deposition of NETs within the lung microvasculature, but depletion of platelets had

[§] Co-Corresponding Authors 1) Allan Tsung, Department of Surgery, The Ohio State University Medical Center, N924 Doan Hall, 410 W. 10th Ave., Columbus, Ohio 43210, USA. Phone: 614-293-8304, allan.tsung@osumc.edu; 2) Hai Huang, Department of Surgery, The Ohio State University Medical Center, N924 Doan Hall, 410 W. 10th Ave., Columbus, Ohio 43210, USA. Phone: 614-293-8235, hai.huang@osumc.edu;.

[†]Co-first Authors

Conflict of Interest Statement The authors declare no conflict of interest.

no effect. TLR4 was essential for platelet activation and platelet-tumor cell aggregate formation in an ERK5-GPIIb/IIIa integrin-dependent manner. Such aggregation facilitated NET-mediated capture of CTCs in vitro under static and dynamic conditions. Blocking platelet activation or knocking out TLR4 protected mice from hepatic I/R-induced metastasis with no CTC-entrapment by NETs. These results uncover a novel mechanism where platelets and neutrophils contribute to metastasis in the setting of acute inflammation. Targeted disruption of the interaction between platelets and NETs holds therapeutic promise to prevent post-operative distant metastasis.

Introduction

Surgery is a long-established, successful intervention strategy that provides a chance for patients to cure or control cancer. However, the perioperative period is characterized by a heightened risk of new metastatic foci at distal sites. Unfortunately, the leading cause of death post-cancer surgery is also recurrence and distant metastasis (1,2). Following surgical removal of primary tumors, the formation of circulating tumor cells (CTCs) represents one of the key events that initiate the metastatic process, serving as seeds of distant tumor formation. As the neoplasm and the associated vessels are disrupted, cancer cells escape and shed into the circulation to form CTCs (3). In addition, surgery also suppresses anti-tumor immunity and enhances migration and invasion of the CTCs to colonize the target organs (4). Therefore, we need a thorough understanding of the molecular mechanisms underlying these pathological processes to develop effective therapeutics (5) and better manage the perioperative period to prevent recurrence and metastasis.

Platelets are one of the early cellular responders to surgical stress and are involved in tissue reparation. Nevertheless, their actions also result in aiding metastasis of the same primary tumor cells (6,7). When CTCs enter into the circulation, platelets quickly shroud them, which shields them from the shear stress of circulation and natural killer cells (8). Additionally, the platelet-released mediators confer new mesenchymal traits to the CTCs, which have been found to promote tumor cell migration and invasion into distant organs (9). Platelets also help tumor cell extravasation by increasing vascular permeability (10). Of note, increasing evidence indicates that antiplatelet agents are capable of impeding tumor metastasis and have shown promising therapeutic benefits for cancer patients (11).

In addition to these contributions to metastasis, platelets also play a role in the dissemination of cancer cells. Recent evidence has implicated an intricate, bidirectional communication between platelets and neutrophil extracellular traps (NETs) in various inflammatory conditions, including bacterial sepsis, transfusion-related acute lung injury (TRALI), and venous thrombosis (12–14). It has been demonstrated that NETs enable neutrophils to ensnare CTCs in experimental models of sepsis, promoting early adhesive events, and facilitating metastatic progression (15). Our own work shows that, during hepatic ischemia/reperfusion (I/R), neutrophils form NETs (16), entrap injected colorectal cancer cells and promote metastasis in the liver (17). However, the interaction between platelets and NETs during the initial phases of surgical stress and the underlying mechanisms of tumor metastasis remain largely unknown. A serious knowledge gap exists, which needs to be

addressed to pave the way for developing perioperative intervention strategies and improve long-term surgical outcomes.

To answer these questions, we chose to use murine hepatic I/R as a model system of acute, non-infectious surgical stress in this study. We show that local hepatic inflammation favors platelet-mediated sequestration of CTCs and subsequent distant metastasis in the lungs. After the entry into the circulation, platelets immediately adhere to the cancer cells and form platelet-CTC aggregates. Our in-depth investigation reveals that this pro-metastatic role of platelets is mediated by TLR4-dependent ERK5-GPIIb/IIIa integrin activation. Further, we find that NETs have a higher affinity for platelet-CTC aggregates than single cancer cells, which enables them to capture CTCs and promote subsequent tumor metastasis. Collectively, these findings uncover a novel mechanism where activated platelets and NETs work together to form micro-metastatic foci in distant organs following local surgical inflammation, leading to cancer recurrence and metastasis.

Materials and Methods

Mice and cell lines

Male C57BL/6 mice (8 to 12-week-old) were purchased from the Jackson Laboratory (Bar Harbor, ME). TLR4 knockout ($TLR4^{-/-}$), TLR4 flox ($TLR4^{loxp/loxp}$), and platelet-specific TLR4-KO ($PF4\text{-}TLR4^{-/-}$) mice were made and bred in Dr. Timory Billiar's laboratory at University of Pittsburgh. Peptidyl arginine deiminase type IV knockout ($PAD4^{-/-}$) mice (18) were bred at our facility. Murine colon carcinoma MC38 cells were obtained from Dr. Michael Lotze (University of Pittsburgh, Pittsburgh, PA). CT26 murine colorectal cancer cells were purchased from ATCC (Manassas, VA). Both cell lines were authenticated using genomic profiling (IDEXX Radil Cell Check). Cells were routinely tested ensure that they were free of mycoplasma using the MycoFluor Mycoplasma Detection Kit (Invitrogen, Carlsbad, CA).

Metastasis model and hepatic ischemia/reperfusion

All animal protocols, including surgical procedures, anesthetics, analgesics, or other medications used were approved by the Animal Care and Use Committee of the Ohio State University and the University of Pittsburgh. Additionally, the experiments were performed in adherence to National Institutes of Health guidelines for the use of laboratory animals. To establish experimental pulmonary metastasis, mice were injected intravenously via the tail veins with MC38 cells or CT26 cells in 100 μl of PBS. Tumor cells were allowed to circulate for 10 minutes. Mice were subjected to I/R with a nonlethal model of segmental (70%) hepatic warm ischemia (1.5 hous) and reperfusion as described previously (16). Sham animals underwent anesthesia, laparotomy, and exposure of the portal triad without hepatic ischemia.

Immunofluorescence staining

Pulmonary specimens were fixed with 4% paraformaldehyde in phosphate-buffered saline (PBS), embedded in O.C.T. compound, and sectioned at a thickness of 8 μm. Lung sections were incubated with antibodies against Ly6G (BD Bioscience), Cit-H3 (Abcam), CD41 (BD

Bioscience), and DAPI (Invitrogen). Large area images in X and Y were obtained thru the Z plane and are presented as a mean intensity projection of Z using a Nikon A1 confocal microscope (purchased with 1S10OD019973–01 awarded to Dr. Simon C. Watkins). Quantification was performed using NIS Elements Software (Nikon).

Quantitation of tumor cells in the target tissue

Lung tissue was mechanically dissociated and then enzymatically digested in a solution of collagenase IV (5 mg/ml) and DNase (100 U/ml) in DMEM for 1 hour at 37 °C. Partially digested tissue was then filtered through a 70 μm cell strainer. Flow cytometry data were acquired using LSRFortessa flow cytometer (Becton Dickinson), and analyzed by Flowjo software (Miltenyi).

Platelet GPIIb/IIIa activation assay

Platelet GPIIb/IIIa activation was determined by using flow cytometry and Alexa Fluor 488-labeled fibrinogen, which specifically binds to activated GPIIb/IIIa. Platelet-rich plasma (PRP) derived from mice underwent hepatic IR or sham procedure were incubated with 15 μg/ml Alexa Fluor 488-labeled fibrinogen at 37 °C for 15 minutes, fixed with 2% paraformaldehyde for 20 minutes, and analyzed by flow cytometry (19).

Determination of cellular aggregates

Platelets, isolated from mice underwent 1.5 hours of partial hepatic ischemia followed by 3 hours of reperfusion or sham procedure, were adjusted to a density of 2×10^7/ml after manually counting with a hemocytometer. Bone marrow-derived neutrophils (1×10^6) were stimulated with 5 μM A23187 at 37°C for 3 hours to induce NETs formation. For incubation with NETs, 1×10^5 MC38 cells were pre-incubated with 2×10^7 platelets for 3 hours and then added to NETs containing tube in a final volume of 1.5 ml at 37°C on a shaking bed incubator for 6 hours. Cells were incubated in staining solution (PBS containing 1% BSA and 2mM EDTA) with specific antibodies at appropriate dilutions for 30 minutes. The cells were then washed with PBS and immediately analyzed by flow cytometry.

Quantitation of NETs

A capture ELISA myeloperoxidase (MPO) associated with DNA was performed to quantitate NETs in mouse serum as described previously (16).

Immunoblotting

Western blot analyses were performed as described previously using whole-cell lysates from either lung tissue or washed platelets (20). Membranes with transferred proteins were incubated overnight with the following antibodies: Cit-H3 (1:800 Abcam), ERK5 (1:800 CST), pERK5 (1:800 CST), p70S6K (1:800 CST), Rac1 (1:800 Abcam) and actin as an internal control.

Platelets depletion and adoptive transfer

Platelet depletion was performed as described previously (21). Briefly, to transiently deplete platelets from mice, 30 μg anti-CD41 antibody (MWReg30, Abcam) were injected

intraperitoneally12 hours before I/R (22). Freshly isolated platelets from wild type or TLR4$^{-/-}$ mice were injected intravenously into platelet-depleted mice at a cell dose of 2 × 10^7 per mice just before tumor injection and hepatic I/R.

Statistical analysis

The data presented in the figures are mean ± SEM (standard error of the mean). Group comparisons were performed using one-way ANOVA with post-hoc Tuker honestly significant difference (HSD) analysis and Student's t-test. Correlations between MPO-DNA levels and the number of tumor cells were examined using the Spearman correlation coefficient. A value of $P<0.05$ was considered to be statistically significant. GraphPad Prism 7 software was used for all statistical analysis and generating graphs.

Results

Surgical stress increases sequestration of CTCs and subsequent distant metastasis

To determine if local inflammatory responses following surgery promote the entrapment of CTCs at potential metastatic sites, we used a highly standardized murine model of partial (70%) hepatic I/R. Mice were administered with 1×10^6 carboxyfluorescein succinimidyl ester (CFSE)-labelled MC38 murine colon carcinoma cells into the systemic circulation via tail vein and followed by a hepatic I/R or sham procedure.

On day 21 post-injection, we found that hepatic I/R mice showed an approximately threefold higher number of metastatic foci on the lung surface relative to sham group ($P<0.001$) (Figure 1A), supporting a vital function of surgical stress in metastasis. Quantification of metastatic foci coverage on hematoxylin and eosin-stained lung tissue sections revealed that the area of metastatic lesion per lung was 53.5% in hepatic I/R group, while only 4.6% in sham group ($P<0.001$) (Figure 1B).

To gain insight into how hepatic I/R causes increased distant metastasis, we enumerated the tumor cells in the lungs of mice underwent hepatic I/R at various time points after tail vein injection. In general, due to the shear force of hemodynamics and attack by the immune system, only a few circulating tumor cells are able to survive and extravasate to form metastasis at distant site (23). Interestingly, no statistical difference in the number of CFSE-labelled MC38 cells was observed in the lungs of hepatic I/R and sham mice within 2 hours after tumor cell injection (Figure 1C). However, at later time points (6 hours, 12 hours, and 24 hours), hepatic I/R led to significant retention of tumor cells (Figure 1C, 1D and 1E). Meantime, a different number of CFSE-labelled MC38 cells were injected into the mice systemic circulation followed by a hepatic I/R or sham procedure. The results were in line with previous results that more tumor cells were sequested in the lungs of mice underwent hepatic I/R (Figure 1F). To extend our obsevations on another tumor cell type, experiments were reiterated by using CT26 murine colorectal cancer cells. The results showed that hepatic I/R led to significant retention of CT26 tumor cells in the lungs of mice (Supplymentary Figure 1A). These data clearly demonstrate that surgical stress-induced by hepatic I/R does not increase the number of CTCs in the lung capillaries, but rather facilitate

better survival of CTCs in the circulation and subsequent colonization in the metastatic process.

Hepatic I/R promotes the formation of platelet-tumor aggregates

The dynamic host-tumor cell interactions during the initial hours after tumor cells enter into the circulation determine the success of distant metastasis (23). Platelets can form aggregates around the tumor cells within a few minutes leading to intravascular survival of tumor cells (24). To determine if platelets activated by surgical stress have a higher affinity for tumor cells, we co-cultured MC38 cells with platelets isolated from mice that underwent hepatic I/R or sham operation. A significant increase in the percentage of tumor cells forming platelet aggregates was observed from hepatic I/R mice (48.6% of the total tumor population), compared to that of control sham mice (21.8% of the total tumor population) ($P<0.01$) (Figure 2A and 2B). In addition, platelet aggregation with MC38 cells increased further when reperfusion time was extended from 1 to 3 hours (61.5% of the total tumor population) ($P<0.05$) (Figure 2A and 2B). These results are not unique to MC38 carcinoma cells, as hepatic I/R also promotes the aggregation of platelets with CT26 cells (Supplumentary Figure 1B).

We next sought to confirm the same results *in vivo*. As shown in Figure 2C, immunofluorescence staining clearly shows the number of CFSE-labelled MC38 cells surrounded by platelets (CD41 positive) was prominently higher in the lungs of mice that underwent hepatic I/R compared to that of sham mice. Remarkably, depletion of platelets by intraperitoneally injecting a platelet-depleting antibody (anti-CD41) before tumor cell injection and hepatic I/R led to a significantly reduced number of tumor cells arrested in the lungs, as compared to isotype antibody treatment ($P<0.0001$) (Figure 2D and 2E). Together, these data indicate that the formation of systemic platelet-tumor cell aggregates after hepatic I/R may contribute to trapping of cancer cells and subsequent distant metastasis in the lungs.

NET-mediated capture requires platelet-tumor cell aggregates

Previously, we found that neutrophils released neutrophil extracellular traps (NETs) in the liver in response to hepatic I/R, and those NETs promoted tumor progression within the liver (17). In this study, we observe a systemic effect of hepatic I/R, and hence, we hypothesized that liver inflammation might also trigger NETs formation at distal sites, including the lungs, to promote the capture of CTCs. To determine NETs formation within the lung tissue after hepatic I/R, we used immunofluorescence staining to probe for NETs. Co-localization of a number of Ly6G-positive cells (a surface marker for murine neutrophils) with extracellular histone and web-like DNA, indicative of NETs formation, was visualized within the lung tissue from mice underwent hepatic I/R (Figure 3A). Furthermore, the expression of citrullination of histone H3 (Cit-H3), a marker of neutrophil extracellular traps (25), increased in the lung tissue when tested after 6, 12, and 24 hours of hepatic I/R in mice (Figure 3B). Circulating myeloperoxidase (MPO)-DNA complexes levels, another specific marker of NETs formation, positively correlated with the number of metastatic tumor cells trapped within the pulmonary microvasculature at 6 hours post-reperfusion (Spearman's coefficient 0.969, $P<0.0001$) (Figure 3C). After disrupting existing NETs with DNase I or inhibiting NETosis by knocking out PAD4, no apparent difference in the number of CTCs in

the pulmonary microvasculature were observed between mice underwent hepatic I/R and sham surgery (Figure 3D). These findings indicate that hepatic I/R-induced inflammation also results in NETs formation in the lungs, which correlates with the retention of CTCs in the pulmonary microvasculature. Next, we explored if activated platelets affect the formation of NETs during hepatic I/R. Mice were treated with platelet-depleting antibodies before operation. Surprisingly, no apparent difference in both the pulmonary expression of Cit-H3 and level of MPO-DNA complexes was detected between anti-CD41 and isotype-treated mice, indicating that NETs formation is platelet independent under surgical stress (Figure 3E and 3F).

We next tested whether activated platelets had any effect on the activities of NETs such as capturing CTCs. Bone marrow-derived neutrophils were stimulated with calcium ionophore A23187 (26) to form NETs, and then incubated with MC38 cells in the presence of platelets derived from mice underwent hepatic I/R or sham surgery. Interaction of Ly6G-positive cells with MC38 cells was studied by flow cytometry as a representation of NET-mediated tumor-cell capture. Compared with the tumor cells arrested in the control group (without platelets, 9.03%), more tumor cells were captured by NETs in the presence of platelets derived from sham surgery mice (17.33%; $P>0.05$) (Figure 4A). Strikingly, the appearance of platelets isolated from hepatic I/R mice resulted in NETs capturing a significantly high percentage of tumor cells (67.82%) ($P<0.001$) (Figure 4A). Consistent with these results, coculture of CT26 tumor cell with platelet I/R also fosters NET-mediated capture of tumor (Supplumentary Figure 1C).

To mimic the *in vivo* circulation and its environment in the laboratory, we simulated with dynamic conditions of flow, and then evaluated the interaction between NETs and tumor cells with or without platelets. A parallel flow chamber was used to perfuse MC38 cells or MC38 pre-incubated with platelets over neutrophil monolayers to simulate pulmonary flow conditions. In line with our observations, following perfusion for 10 minutes, a significantly high number of tumor cells were trapped by NETs when pre-incubated with platelets isolated from hepatic I/R mice ($P<0.001$) (Figure 4B and Supplementary Movies). In contrast, pretreatment of MC38 with platelets derived from sham mice had no effect on NET-trapping MC38 cells (Figure4C). Consistent results were obtained under a static system, where tumor cells were transiently co-cultured with or without platelet on a NET-coated plate (Figure 4D).

The enhanced entrapment of platelets-tumor cell aggregates within NETs implies that platelets may stimulate tumor cells migration towards NETs. We sought to test this directly *in vitro* by transwell migration assays. NETs were pre-induced with A23187 in the lower chamber. Then the treated MC38 cells in FBS-free medium were seed onto the upper chamber. The results showed that, compared with the control group (without platelets, 185/per field), more MC38 cells migrated through pores in the presence of sham platelets (219/per field; $P<0.05$). Moreover, the migration ability of MC38 cells significantly increased in the presence of platelets derived from I/R mice (435/per field; $P<0.001$) (Figure 4E). Taken together, these results indicate that NETs are prone to capture platelet-CTC aggregates.

Aggregation of platelets with CTCs and distant metastasis after hepatic I/R stress is platelet ERK5-dependent

We next focused on dissecting the mechanisms of platelet activation in response to surgical stress. Reactive oxygen species (ROS), a hallmark of I/R injury, has been shown to be responsible for platelet activation via extracellular-regulated protein kinase 5 (ERK5) in myocardial infarction (27,28). We, therefore, evaluated the role of ERK5 during hepatic I/R in activating platelets. Platelets derived from mice underwent hepatic I/R had elevated expression of phosphorylated ERK5 at Thr 218 and Thr 220, and a significantly elevated ratio of pERK5/ERK5 than those of sham surgery (Figure 5A). Furthermore, hepatic I/R also dramatically increased the expression of downstream 70-kDa ribosomal S6 kinase (P70S6K) and Ras-related C3 botulinum toxin substrate 1 (Rac1) in platelets (Figure 5A), two integral signal transduction components required for integrin activation (29).

Activated platelets are known to interact with tumor cells through a variety of surface molecules. Integrins (mainly GPIIb/IIIa) and P-selection are the two well-known platelet surface proteins responsible for binding tumor cells (30,31). We used Alexa Fluor 488-labeled fibrinogen, which specifically binds to activated GPIIb/IIIa, to examine the status of Integrin protein. Supplementary Figure 2A shows that activation of platelet GPIIb/IIIa is more pronounced in I/R mice than in sham mice (2092 MFI [1126–2976] *vs.* 811 MFI [693–984], $P<0.01$). However, no significant difference in P-selectin expression was detected between the platelets of the experimental and control mice (Supplementary Figure 2B).

We further explored whether the potent pharmacological inhibitor of ERK5 signaling (32), XMD8–92, reduces hepatic I/R induced-GPIIb/IIIa activation, platelet-tumor aggregation, and CTCs lung metastasis. As expected, XMD8–92 significantly reduced ERK5 phosphorylation in platelets from hepatic I/R. The expression of P70S6K/RAC1 and activation of GPIIb/IIIa were greatly reduced after treatment with XMD8–92 (Figure 5B and 5C). XMD8–92 pretreatment abolished hepatic I/R-induced formation of platelet-tumor aggregates (Figure 5D). Additionally, pretreatment with XMD8–92 dramatically impaired the seeding of CTCs to the lungs of mice by approximately 90% as compared with the mice exposed to vehicle ($P<0.001$) (Figure 5E and 5F).

To investigate whether ERK5 signaling inhibits NETs formation, we measured MPO-DNA complexes and the pulmonary expression of Cit-H3, respectively. Consistent with our observations above, no significant difference was seen in the serum level of circulating MPO-DNA complexes, as well as the pulmonary expression of Cit-H3 between vehicle and XMD8–92-treatment groups following hepatic I/R (Figure 5G and 5H). This further supports our findings that platelet responses to surgical stress might not directly involve NETs formation, but later at entrapping the CTCs. Collectively, these data demonstrate that the platelet ERK5-GPIIb/IIIa signaling pathway plays a vital role in platelet activation and platelet-tumor cell aggregation during hepatic I/R.

Platelet TLR4 is essential for activation of platelet ERK5 to mediate NETs capturing of tumor cells

Currently, the signaling pathway leading to the activation of ERK5 during surgical stress is unknown. Platelets have toll-like receptors on the surface that enable pathogen recognition. It has been reported that platelet TLR4 is an essential mediator of the inflammatory response as well as platelet activation in hemorrhagic shock (33,34). Therefore, we hypothesized that activation of platelet ERK5 and the formation of platelet-CTC aggregates following hepatic I/R are induced by TLR4. Platelets were isolated from mice with platelet-specific TLR4 ablation (PF4-TLR4$^{-/-}$) or TLR4$^{loxp/loxp}$ mice, both underwent hepatic I/R. Genetic deletion of TLR4 almost completely abolished the upregulation of pERK5/P70S6K/RAC1 (Figure 6A). To further confirm the role of TLR4 on the ERK5 pathway, we used anti-CD41 to deplete platelet in the above mice. Platelets obtained from wild type and TLR4$^{-/-}$ mice were then adoptively transferred into platelets-depleted mice followed by tumor cell injection and hepatic I/R. In contrast to TLR4$^{-/-}$ platelets, adoptive transfer of wild type platelets resulted a significant increase in the expression of phosphorylated ERK5 and downstream P70S6K and RAC1 (Figure 6B). These data indicate that platelet TLR4 is essential for surgery-induced activation of ERK5/ P70S6K/RAC1 pathway. Concurrently, the activation of integrin GPIIb/IIIa and platelet-tumor cell aggregation was also inhibited in PF4-TLR4$^{-/-}$ mice that underwent hepatic I/R (Figure 6C and 6D). These data indicated that platelet TLR4 signaling as a key upstream trigger of ERK5/P70S6K/Rac1 is essential for the activation of platelets and the formation of platelet-tumor aggregates.

Our above data indicates that platelet TLR4 acts upstream of the ERK5-integrin pathway. We then explored the possibility that the TLR4 gene ablation could also affect the NET-mediated capture of tumor cells. Calcium ionophore A23187 was used to stimulate NETs formation in neutrophil monolayers. MC38 cells pre-incubated with platelets from PF4-TLR4$^{-/-}$ and TLR4$^{loxp/loxp}$ mice that underwent hepatic I/R were perfused over neutrophil monolayers as described above. As expected, the pro-adhesive effect of platelets on NET-mediated tumor cell capture was reduced when TLR4 was absent in the dynamic adhesion system *in vitro* (Figure 6E). Consistent results were obtained under a static system, where tumor cells were transiently co-cultured with platelets from PF4-TLR4$^{-/-}$ and TLR4$^{loxp/loxp}$ mice that underwent hepatic I/R or without platelets on a NET-coated plate (Figure 6F and 6G). Together, these results showed that the genetic deletion of TLR4 in platelets abolished the pro-adhesive effect of platelets on NET-mediated tumor cell capture *in vitro*.

We also examined the effect of TLR4 on NETs formation following hepatic I/R. The results showed no significant difference in the serum level of circulating MPO-DNA complexes, as well as pulmonary expression of Cit-H3, in PF4-TLR4$^{-/-}$ and TLR4$^{loxp/loxp}$ mice (Figure 6H and 6I). Altogether, these data suggest that selective deletion of platelet TLR4 does not affect NETs formation, but rather on the ERK-signaling pathway leading to the activation of platelets and NET-mediated capturing of CTCs.

The mechanism by which activates platelets TLR4-ERK5 signaling after hepatic I/R remains elusive. We have previously reported that endogenous molecules released from stressed hepatocytes during hepatic I/R, such as High Mobility Group Box 1 (HMGB1) and histones, invoke an inflammatory response (16). Therefore, we next determined whether exogenous

HMGB1 or histones could trigger platelet TLR4-ERK5 signaling. We found that both recombinant HMGB1 and histones dramatically increased the expression of pERK5/P70S6K/RAC1 in wild type platelets *in vitro*, but not in $TLR4^{-/-}$ platelets (Figure 6J). These results suggest that engagement of TLR4 with its ligands plays a fundamental role in activation of platelet ERK5 to mediate NETs capturing of tumor cells.

Platelet TLR4 facilitates surgical stress-induced metastasis *in vivo*

To confirm the above *in vitro* findings, platelets obtained from WT or $TLR4^{-/-}$ mice were adoptively transferred into platelets-depleted WT mice followed by tumor cell injection and hepatic I/R (Supplementary Figure 3A). Compared to WT platelets, adoptive transfer of $TLR4^{-/-}$ platelets resulted in significantly fewer lung metastasis mice adoptive transferred with ($P<0.01$) (Supplementary Figure 3B and 3C).

To further confirm the role of platelet TLR4 in post-operative distant metastasis *in vivo*, we used PF4-$TLR4^{-/-}$ and $TLR4^{loxp/loxp}$ mice. The selective deletion of TLR4 in platelets contributed to a significant reduction of lung tumors compared to $TLR4^{loxp/loxp}$ control mice ($P<0.01$) (Figure 7A and B). Importantly, the 21-day metastatic burden, as described above, was significantly reduced in the PF4-$TLR4^{-/-}$compared with $TLR4^{loxp/loxp}$ mice (Figure 7C, 7D and 7E). Taken together, our data indicate that platelet TLR4 is a promising target for preventing NET-driven distant metastasis (Figure 7F).

Discussion

Accumulating evidence indicates that the host immune cells are crucial in driving tumor progression and distant metastasis (11,35–38). Only a fraction of CTCs is capable of surviving within the vasculature, succeeding in extravasation, and metastatic dissemination. Navigation through the stress factors and colonizing at distant organs are also key to metastasis. The behavior of CTCs is highly influenced by their microenvironment, especially the presence of host immune cells in the circulatory system (39). This work delineates how two initial responders of the innate immunity, platelets and neutrophils, engage in a well-orchestrated interaction with CTCs to promote distant metastasis under surgical stress. Such effects stand proof that drastic changes in the systemic physiology of hosts influence various aspects of pathology, including the invasion-metastatic cascade.

In this study, we show that surgical stress activates platelets through ERK5/integrin GPIIb/IIIa signaling, leading to increased aggregation of platelets with CTCs. Previous reports have suggested that platelets surround tumor cells very rapidly and the aggregates localize to the site within 1 minute of tumor cell entry into the circulation, which is essential for the early metastatic niche formation and subsequent metastasis (24). In this ‘pre-metastatic niche’ model, the platelet-tumor cell interaction recruits granulocytes, which, in turn, support metastatic seeding (24). While several adhesion molecules, including integrins, selectins, and their ligands, have been shown to contribute to the interaction of platelets with tumor cells, integrin GPIIb/IIIa is especially efficient in this regard. We present evidence here that in local I/R, ERK5 in the platelets is immediately phosphorylated, and its activity results in conferring CTC-adhesion property to the platelets mainly via activated integrin GPIIb/IIIa. The robust response from this pathway implies that other signaling pathways and molecules

might be involved in platelet activation and its adhesion property, but only to a lesser degree. These findings warrant further investigation of potent pharmacological inhibitors of ERK5 signaling in order to disrupt the surgery-induced platelet activation and subsequent platelet-tumor cell aggregation.

Toll-like receptors on the surface of platelets contribute to pathogen recognition making platelets as one of the main components of innate immunity (40). TLR4 membrane receptor, in particular, is known to play a major role in experimental tumor metastasis of murine B16F10 melanoma and Lewis lung carcinoma cells via interaction with tumor cell-released HMGB1 (41). These studies suggest that targeting platelet TLR4 is an effective approach to treating cancer metastasis. The effect of TLR4 on metastatic promotion observed in tumor-bearing mice (41) and our findings that platelet TLR4 plays a crucial role in metastasis in mice underwent hepatic I/R are consistent. By using platelet-specific knockout mice, we delineated the metastatic cascade where platelet TLR4, after surgical stress, leads to phosphorylation of ERK5 that results in activating platelets and promoting their aggregation with CTCs through surface integrin GPIIb/IIIa.

TLR4 is highly expressed in malignant cells and a variety of host cells within the tumor, including endothelial cells, fibroblasts, immune cells, and a variety of precursor cells recruited to the tumor inflammatory environment by TLR4-dependent chemokines. In these nucleated cells, TLR4 is well-known to activate intracellular signaling pathway via NF-κB, which result in upregulation of inflammatory cytokines, pro-survival and migratory factors (42). TLR4-induced inflammation has been shown to promote tumor growth, vasularization and metastasis. Although platelets lack genomic DNA, they are equipped with RNA splicing machineries that process resident pre-mRNAs to store performed and synthesized immunomodulatory molecules, including platelet-derived growth factor, IL-1β and CCL5 in response to infectious or sterile insults (43). Thus, therapeutic targeting of platelet TLR4 may have the potential to reverse tumour-supporting inflammation and to inhibit metastatic spread.

Apart from forming aggregates with CTCs and protecting them from shear stress, activated platelets have been shown to directly induce NETs formation, and those NETs can increase endothelial permeability in the lungs of experimental mice underwent TRALI (13). Initially identified as a fundamental host innate immune defense against pathogens, the actions of NETs were later found to contribute to harmful inflammation as well as tissue injury and tumor metastasis (17,44,45). In this study, we find significantly increased NETs formation in the lung microcirculation and abundant NETs components in the plasma in experimental surgical stress, which enhances their ability to sequester CTCs and induce distant metastasis. However, platelet depletion before IR surgery did not affect the formation of NETs and their deposition in the lung tissue, indicating that the pro-metastatic role of activated platelets does not impact on NETs formation. In our previous study, we have unraveled the mechanism by which hepatic I/R triggers neutrophil activation and NETs formation. During hepatic surgery, the release of damage-associated molecular patterns (DAMPs) from stressed hepatocytes, including HMGB1 and histone, trigger NETs formation via the TLR-dependent pathways (16).

NETs were first defined as facilitators of tumor progression in the context of post-operative sepsis (46). During settings of severe infection, NETs are able to trap CTCs promoting intravascular survival and early adhesion of tumor cells to distant organ sites. Along this line, the pivotal role of NETs in the metastatic cascade has been demonstrated both in experimental tumor-bearing mice and clinical studies, and it is believed that they hold a strong potential for novel strategies in the therapeutic management of metastatic diseases (47–49). Their mechanistic analysis reveals that the adhesion between NETs and CTCs is either a protein-protein interaction mediated by integrins (50) or NETs DNA with transmembrane protein CCDC25 on cancer cells (48). Here, we demonstrate a different mechanism where platelets act as a bridge, tethering CTCs to the NETs deposited in the lungs after systemic inflammation induced by surgery stress.

In conclusion, our work demonstrates that platelets facilitate NET-mediated capture of CTCs and subsequent metastasis in the context of surgical stress. In the microvasculature, the new TLR4-ERK5-integrin GPIIb/IIIa axis leads to platelet activation and formation of microaggregates with tumor cells in the early stages of reperfusion. These complexes were then recruited to the NETs within the capillary bed of specific organs, causing the formation of metastatic foci in those target organs. Blockade of TLR4 on platelets or of ERK5-dependent platelet-tumor aggregates show promise in preventing surgery-driven distant metastasis. As surgical resection of solid tumors becomes increasingly routine, our study may open new avenues for improving clinical outcomes for patients post-resection.

Supplementary Material

Refer to Web version on PubMed Central for supplementary material.

Acknowledgment

A.T. is supported by grants from National Institute of Health/National Cancer Institute (NCI) (R01-CA214865-01) and National Institutes of Health/National Institute of Genernal Medical Sciences (NIGMS) (R01-GM95566-06). H.H. is supported by Joesph A. Patrick Research Fellowship in Transplantation and the grant from National Institutes of Health/National Institute of Genernal Medical Sciences (NIGMS) (R01-GM137203). J.R. is supported by National Natural Science Foundation of China (NSFC) (81874084 and 82072800). The authors thank Xinghua Liao for technical assistance in preparing the manuscript.

References

1. Krall JA, Reinhardt F, Mercury OA, Pattabiraman DR, Brooks MW, Dougan M, et al. The systemic response to surgery triggers the outgrowth of distant immune-controlled tumors in mouse models of dormancy. Science translational medicine 2018;10
2. Wang T, Wang D, Yu H, Feng B, Zhou F, Zhang H, et al. A cancer vaccine-mediated postoperative immunotherapy for recurrent and metastatic tumors. Nat Commun 2018;9:1532 [PubMed: 29670088]
3. Martin OA, Anderson RL, Narayan K, MacManus MP. Does the mobilization of circulating tumour cells during cancer therapy cause metastasis? Nature reviews Clinical oncology 2017;14:32–44
4. Tohme S, Simmons RL, Tsung A. Surgery for Cancer: A Trigger for Metastases. Cancer Res 2017;77:1548–52 [PubMed: 28330928]
5. Kitamura T, Qian BZ, Pollard JW. Immune cell promotion of metastasis. Nature reviews Immunology 2015;15:73–86
6. Gay LJ, Felding-Habermann B. Contribution of platelets to tumour metastasis. Nature reviews Cancer 2011;11:123–34 [PubMed: 21258396]

7. Palumbo JS, Talmage KE, Massari JV, La Jeunesse CM, Flick MJ, Kombrinck KW, et al. Platelets and fibrin(ogen) increase metastatic potential by impeding natural killer cell-mediated elimination of tumor cells. Blood 2005;105:178–85 [PubMed: 15367435]
8. Tesfamariam B Involvement of platelets in tumor cell metastasis. Pharmacol Ther 2016;157:112–9 [PubMed: 26615781]
9. Labelle M, Begum S, Hynes RO. Direct signaling between platelets and cancer cells induces an epithelial-mesenchymal-like transition and promotes metastasis. Cancer cell 2011;20:576–90 [PubMed: 22094253]
10. Ward Y, Lake R, Faraji F, Sperger J, Martin P, Gilliard C, et al. Platelets Promote Metastasis via Binding Tumor CD97 Leading to Bidirectional Signaling that Coordinates Transendothelial Migration. Cell reports 2018;23:808–22 [PubMed: 29669286]
11. Xu XR, Yousef GM, Ni H. Cancer and platelet crosstalk: opportunities and challenges for aspirin and other antiplatelet agents. Blood 2018;131:1777–89 [PubMed: 29519806]
12. Clark SR, Ma AC, Tavener SA, McDonald B, Goodarzi Z, Kelly MM, et al. Platelet TLR4 activates neutrophil extracellular traps to ensnare bacteria in septic blood. Nat Med 2007;13:463–9 [PubMed: 17384648]
13. Caudrillier A, Kessenbrock K, Gilliss BM, Nguyen JX, Marques MB, Monestier M, et al. Platelets induce neutrophil extracellular traps in transfusion-related acute lung injury. J Clin Invest 2012;122:2661–71 [PubMed: 22684106]
14. Martinod K, Wagner DD. Thrombosis: tangled up in NETs. Blood 2014;123:2768–76 [PubMed: 24366358]
15. Cools-Lartigue J, Spicer J, McDonald B, Gowing S, Chow S, Giannias B, et al. Neutrophil extracellular traps sequester circulating tumor cells and promote metastasis. The Journal of clinical investigation 2013;123:3446–58
16. Huang H, Tohme S, Al-Khafaji AB, Tai S, Loughran P, Chen L, et al. Damage-associated molecular pattern-activated neutrophil extracellular trap exacerbates sterile inflammatory liver injury. Hepatology 2015;62:600–14 [PubMed: 25855125]
17. Tohme S, Yazdani HO, Al-Khafaji AB, Chidi AP, Loughran P, Mowen K, et al. Neutrophil Extracellular Traps Promote the Development and Progression of Liver Metastases after Surgical Stress. Cancer Res 2016;76:1367–80 [PubMed: 26759232]
18. Hemmers S, Teijaro JR, Arandjelovic S, Mowen KA. PAD4-mediated neutrophil extracellular trap formation is not required for immunity against influenza infection. PLoS One 2011;6:e22043 [PubMed: 21779371]
19. Schmaier AA, Zou Z, Kazlauskas A, Emert-Sedlak L, Fong KP, Neeves KB, et al. Molecular priming of Lyn by GPVI enables an immune receptor to adopt a hemostatic role. Proceedings of the National Academy of Sciences 2009;106:21167–72
20. van der Windt DJ, Sud V, Zhang H, Varley PR, Goswami J, Yazdani HO, et al. Neutrophil extracellular traps promote inflammation and development of hepatocellular carcinoma in nonalcoholic steatohepatitis. Hepatology 2018;68:1347–60 [PubMed: 29631332]
21. Zhang H, Goswami J, Varley P, van der Windt DJ, Ren J, Loughran P, et al. Hepatic Surgical Stress Promotes Systemic Immunothrombosis That Results in Distant Organ Injury. Front Immunol 2020;11:987 [PubMed: 32528475]
22. Goncalves R, Zhang X, Cohen H, Debrabant A, Mosser DM. Platelet activation attracts a subpopulation of effector monocytes to sites of Leishmania major infection. The Journal of experimental medicine 2011;208:1253–65 [PubMed: 21606505]
23. Labelle M, Hynes RO. The initial hours of metastasis: the importance of cooperative host-tumor cell interactions during hematogenous dissemination. Cancer Discov 2012;2:1091–9 [PubMed: 23166151]
24. Labelle M, Begum S, Hynes RO. Platelets guide the formation of early metastatic niches. Proc Natl Acad Sci U S A 2014;111:E3053–61 [PubMed: 25024172]
25. Leshner M, Wang S, Lewis C, Zheng H, Chen XA, Santy L, et al. PAD4 mediated histone hypercitrullination induces heterochromatin decondensation and chromatin unfolding to form neutrophil extracellular trap-like structures. Front Immunol 2012;3:307 [PubMed: 23060885]

26. Douda DN, Khan MA, Grasemann H, Palaniyar N. SK3 channel and mitochondrial ROS mediate NADPH oxidase-independent NETosis induced by calcium influx. Proc Natl Acad Sci U S A 2015;112:2817–22 [PubMed: 25730848]
27. Tsung A, Klune JR, Zhang X, Jeyabalan G, Cao Z, Peng X, et al. HMGB1 release induced by liver ischemia involves Toll-like receptor 4–dependent reactive oxygen species production and calcium-mediated signaling. Journal of Experimental Medicine 2007;204:2913–23
28. Cameron SJ, Ture SK, Mickelsen D, Chakrabarti E, Modjeski KL, McNitt S, et al. Platelet Extracellular Regulated Protein Kinase 5 Is a Redox Switch and Triggers Maladaptive Platelet Responses and Myocardial Infarct Expansion. Circulation 2015;132:47–58 [PubMed: 25934838]
29. Aslan JE, Tormoen GW, Loren CP, Pang J, McCarty OJ. S6K1 and mTOR regulate Rac1-driven platelet activation and aggregation. Blood 2011;118:3129–36 [PubMed: 21757621]
30. Chen M, Geng JG. P-selectin mediates adhesion of leukocytes, platelets, and cancer cells in inflammation, thrombosis, and cancer growth and metastasis. Arch Immunol Ther Exp (Warsz) 2006;54:75–84 [PubMed: 16648968]
31. Lavergne M, Janus-Bell E, Schaff M, Gachet C, Mangin PH. Platelet Integrins in Tumor Metastasis: Do They Represent a Therapeutic Target? Cancers (Basel) 2017;9
32. Finegan KG, Perez-Madrigal D, Hitchin JR, Davies CC, Jordan AM, Tournier C. ERK5 Is a Critical Mediator of Inflammation-Driven Cancer. Cancer research 2015;75:742–53 [PubMed: 25649771]
33. Vallance TM, Zeuner MT, Williams HF, Widera D, Vaiyapuri S. Toll-Like Receptor 4 Signalling and Its Impact on Platelet Function, Thrombosis, and Haemostasis. Mediators Inflamm 2017;2017:9605894 [PubMed: 29170605]
34. Wang G, Hu Z, Fu Q, Song X, Cui Q, Jia R, et al. Resveratrol mitigates lipopolysaccharide-mediated acute inflammation in rats by inhibiting the TLR4/NF-kappaBp65/MAPKs signaling cascade. Sci Rep 2017;7:45006 [PubMed: 28322346]
35. Wculek SK, Malanchi I. Neutrophils support lung colonization of metastasis-initiating breast cancer cells. Nature 2015;528:413–7 [PubMed: 26649828]
36. Liang W, Li Q, Ferrara N. Metastatic growth instructed by neutrophil-derived transferrin. Proc Natl Acad Sci U S A 2018;115:11060–5 [PubMed: 30301793]
37. Schumacher D, Strilic B, Sivaraj KK, Wettschureck N, Offermanns S. Platelet-derived nucleotides promote tumor-cell transendothelial migration and metastasis via P2Y2 receptor. Cancer Cell 2013;24:130–7 [PubMed: 23810565]
38. Haemmerle M, Stone RL, Menter DG, Afshar-Kharghan V, Sood AK. The Platelet Lifeline to Cancer: Challenges and Opportunities. Cancer Cell 2018;33:965–83 [PubMed: 29657130]
39. Massague J, Obenauf AC. Metastatic colonization by circulating tumour cells. Nature 2016;529:298–306 [PubMed: 26791720]
40. Prakash P, Kulkarni PP, Lentz SR, Chauhan AK. Cellular fibronectin containing extra domain A promotes arterial thrombosis in mice through platelet Toll-like receptor 4. Blood 2015;125:3164–72 [PubMed: 25700433]
41. Yu LX, Yan L, Yang W, Wu FQ, Ling Y, Chen SZ, et al. Platelets promote tumour metastasis via interaction between TLR4 and tumour cell-released high-mobility group box1 protein. Nat Commun 2014;5:5256 [PubMed: 25348021]
42. Kawai T, Akira S. The role of pattern-recognition receptors in innate immunity: update on Toll-like receptors. Nat Immunol 2010;11:373–84 [PubMed: 20404851]
43. Semple JW, Italiano JE Jr., Freedman J. Platelets and the immune continuum. Nat Rev Immunol 2011;11:264–74 [PubMed: 21436837]
44. Brinkmann V, Reichard U, Goosmann C, Fauler B, Uhlemann Y, Weiss DS, et al. Neutrophil extracellular traps kill bacteria. Science 2004;303:1532–5 [PubMed: 15001782]
45. Korkmaz B, Horwitz MS, Jenne DE, Gauthier F. Neutrophil elastase, proteinase 3, and cathepsin G as therapeutic targets in human diseases. Pharmacol Rev 2010;62:726–59 [PubMed: 21079042]
46. Cools-Lartigue J, Spicer J, McDonald B, Gowing S, Chow S, Giannias B, et al. Neutrophil extracellular traps sequester circulating tumor cells and promote metastasis. J Clin Invest 2013

47. Teijeira A, Garasa S, Gato M, Alfaro C, Migueliz I, Cirella A, et al. CXCR1 and CXCR2 Chemokine Receptor Agonists Produced by Tumors Induce Neutrophil Extracellular Traps that Interfere with Immune Cytotoxicity. Immunity 2020;52:856–71 e8 [PubMed: 32289253]

48. Yang L, Liu Q, Zhang X, Liu X, Zhou B, Chen J, et al. DNA of neutrophil extracellular traps promotes cancer metastasis via CCDC25. Nature 2020;583:133–8 [PubMed: 32528174]

49. Albrengues J, Shields MA, Ng D, Park CG, Ambrico A, Poindexter ME, et al. Neutrophil extracellular traps produced during inflammation awaken dormant cancer cells in mice. Science 2018;361

50. Najmeh S, Cools-Lartigue J, Rayes RF, Gowing S, Vourtzoumis P, Bourdeau F, et al. Neutrophil extracellular traps sequester circulating tumor cells via beta1-integrin mediated interactions. Int J Cancer 2017;140:2321–30 [PubMed: 28177522]

Statement of significance

Targeting platelet activation via TLR4/ERK5/integrin GPIIb/IIIa signaling shows potential for preventing NET-driven distant metastasis in patients post-resection.

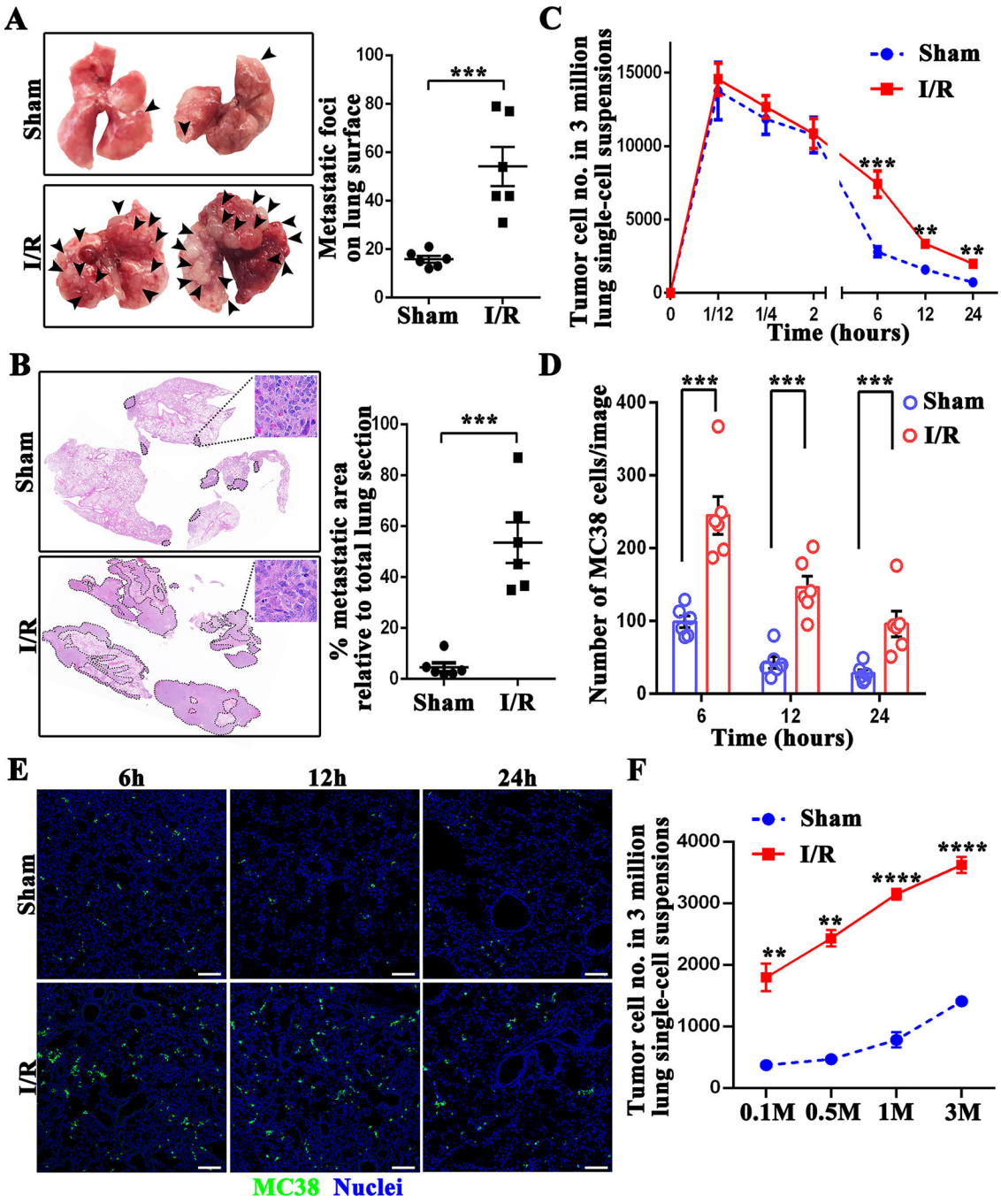

Figure 1.

Surgical stress augments metastatic colonization. (A) Representative images show metastatic pulmonary nodules at day 21 following tumor cell injection in mice subjected to sham or hepatic I/R group. (B) Representative images of H&E staining of lung sections after necropsy in mice subjected to sham or hepatic I/R group. Pathological sections revealed that tumor cells were loosely arranged, with extreme nuclear pleomorphism, hyperchromatic nuclei and nuclear fission. Tumor burden was measured as percent lung tissue replaced by metastatic tumor. (C) Lung tissues were collected at the indicated time after the injection of

10^6 MC38 cells followed by hepatic I/R or sham surgery. The number of tumor cells in a 3 million lung single-cell suspension was determined by FACS. (D) Quantitation of tumor cells in mouse lungs at 6, 12, and 24 hours after MC38 injection in mice subjected to hepatic I/R compared with the sham group. Points represent the mean ± SEM (n ≥ 9 images). (E) Representative immunofluorescence images by confocal microscopy of mice lung sections showing tumor cells at the times indicated following the injection of MC38 cells. Green: MC38; Blue: Nuclei. Scale bar, 100μm. (F) Lung tissues were collected at 12 hours after the injection of different dose of MC38 cells (10^5, 5×10^5, 10^6 and 3×10^6) followed by hepatic I/R or sham surgery. The number of tumor cells in a 3 million lung single-cell suspension was determined by FACS. Data are presented as mean ± SEM from n = 3–6 mice per group. ** $P<0.01$, *** $P<0.001$ and **** $P<0.0001$.

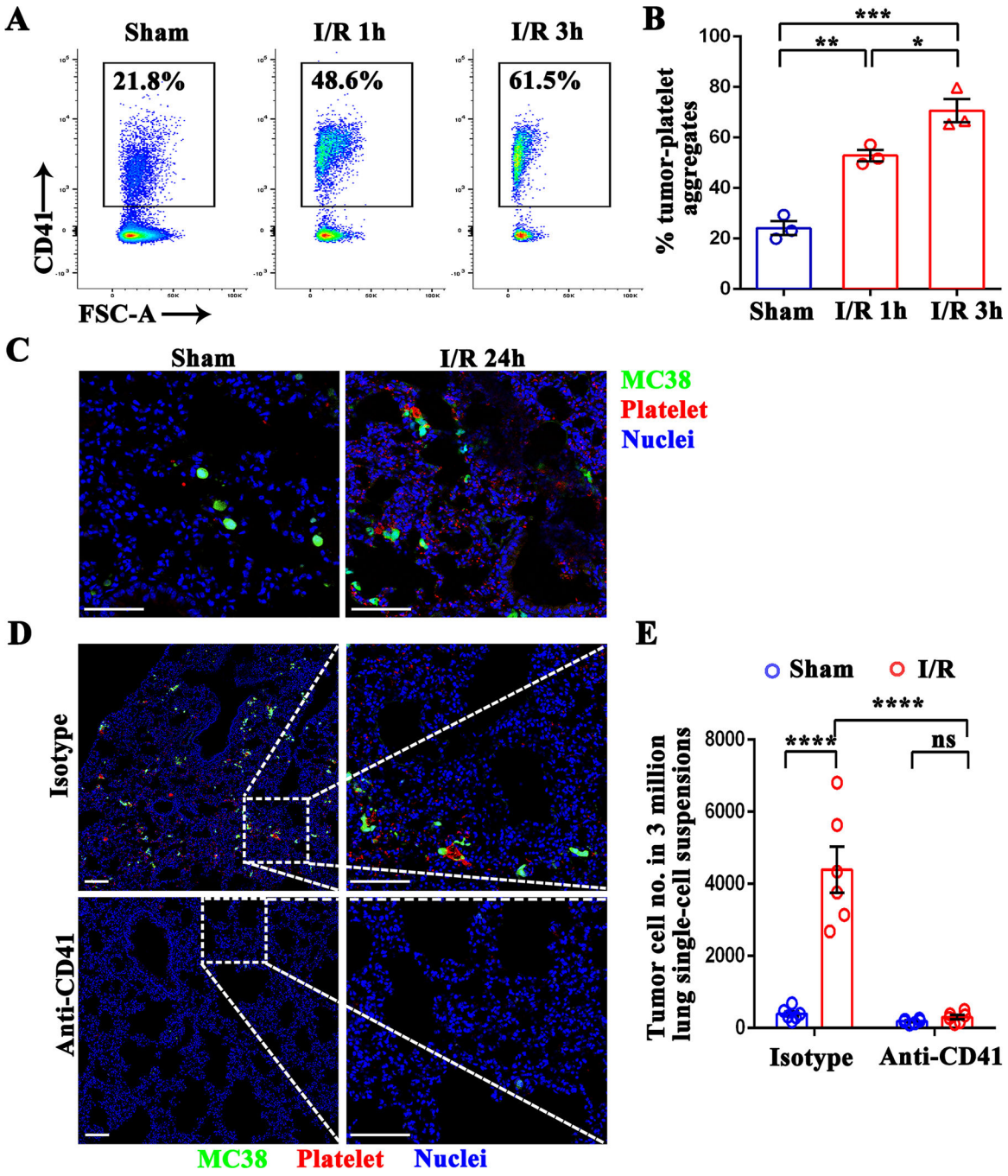

Figure 2.

Hepatic I/R promotes the formation of platelet-tumor cell aggregates and subsequent distant metastasis. (A) Representative flow cytometry showing platelet-tumor cell aggregates. Following 1.5 hours of hepatic ischemia and 1 or 3 hours of reperfusion, platelets were extracted from I/R or sham mice, and then co-cultured with CFSE-labeled MC38 for 10 minutes. (B) From the flow cytometry results in A, platelet-MC38 aggregates were calculated as a percentage of total cancer cells. (C) Representative immunofluorescence images showing colocalization pattern between tumor cells and platelets at 24 hours post-

injection. Platelets were stained with anti-CD41-PE. Green: MC38; Red: platelet; Blue: Nuclei. Scale bar, 100μm. (D) WT mice were injected intraperitoneally with either platelet-depleting anti-CD41 antibody or IgG isotype followed by tumor cell injection and hepatic I/R. Representative immunofluorescence images by confocal microscopy of mice lung sections showing tumor cells arrested at 24 hours post-injection. Green: MC-38; Red: Platelet; Blue: Nuclei. Scale bar, 100μm. (E) FACS quantitative data of MC38 cell numbers in the lungs of mice at 12 hours post-injection. Data are presented as mean ± SEM from n = 3–6 mice per group. ns: not significant, * $P<0.05$, ** $P<0.01$, *** $P<0.001$ and **** $P<0.0001$.

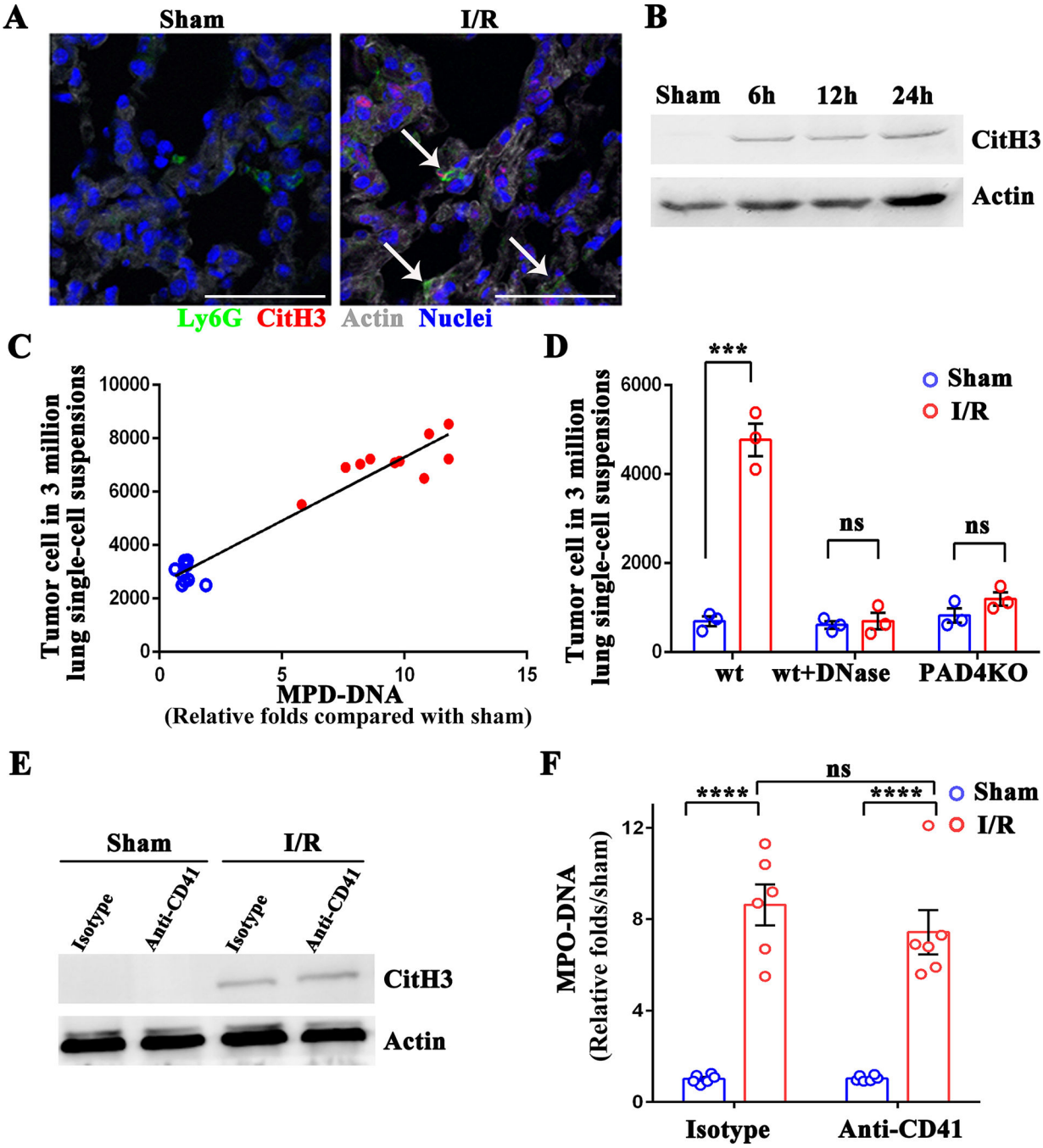

Figure 3.

NETs formation in the lung during hepatic I/R is platelet-independent. (A) Representative immunofluorescence images by confocal microscopy showing NETs formation in the lung sections of mice after 1.5 hours of ischemia and 6 hours of reperfusion. Green: Ly6G; Red: Cit-H3; Gray: Actin; Blue: Nuclei. Arrow: released histone and DNA from the neutrophils. Scale bar, 100μm. (B) NETs formation in the lungs after 1.5 hours of ischemia followed by 6, 12, and 24 hours of reperfusion, as assessed by western blot analysis of Cit-H3 protein levels. (C) The correlation of MC38 cells arrested in the lung tissue at 6 hours post-hepatic

I/R (solid red circles) or sham (hollow blue circles) with its serum level of MPO-DNA. (D) FACS quantitative data of MC38 cell numbers in lungs of mice at 12 hours post-injection in the lung of PAD4 deficient mice and in mice treated with DNase I. (E) The level of Cit-H3 protein was determined by western blot analysis in control or anti-CD41-treated mice after either sham laparotomy or 1.5 hours of ischemia and 6 hours of reperfusion. (F) Serum MPO-DNA complex levels were assessed in control or anti-CD41-treated mice in E. Data are presented as mean ± SEM from n = 3–10 mice per group. ns: not significant, *** $P<0.001$ and **** $P < 0.0001$.

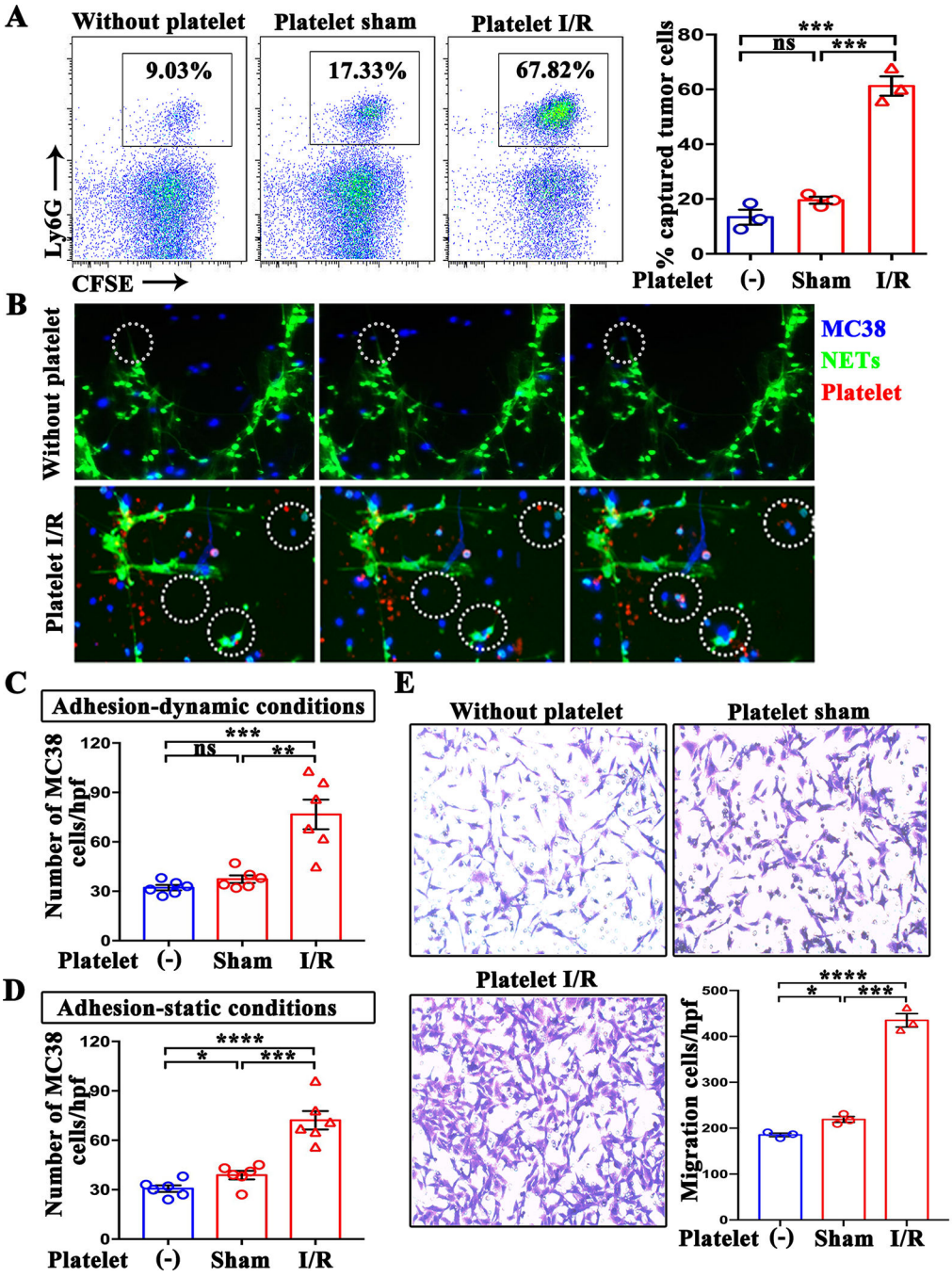

Figure 4.

The formation of platelet-tumor cell aggregates is necessary for NET-mediated capture. (A) Representative flow cytometry plots of NET-captured tumor cells in an *in vitro* co-culture setting in the presence and absence of platelets. (B) Time course of tumor cell adhesion to NETs in the presence and absence of platelets under dynamic conditions. Blue: MC38; green: NETs; red: Platelet. (C and D) Quantitation of tumor cells that adhered to NETs under dynamic and static conditions. Quantitation was performed by counting the number of cells from 6 images per experiment (×20). (E) The migration rates of MC38 towards NETs

in the presence and absence of platelets were measured by transwell migration assays. The number of migrated cells were counted in 6 images per experiment (×20). Data from three or more independent experiments are presented as mean ± SEM. ns: not significant, * $P<0.05$, ** $P<0.01$, *** $P<0.001$ and **** $P < 0.0001$.

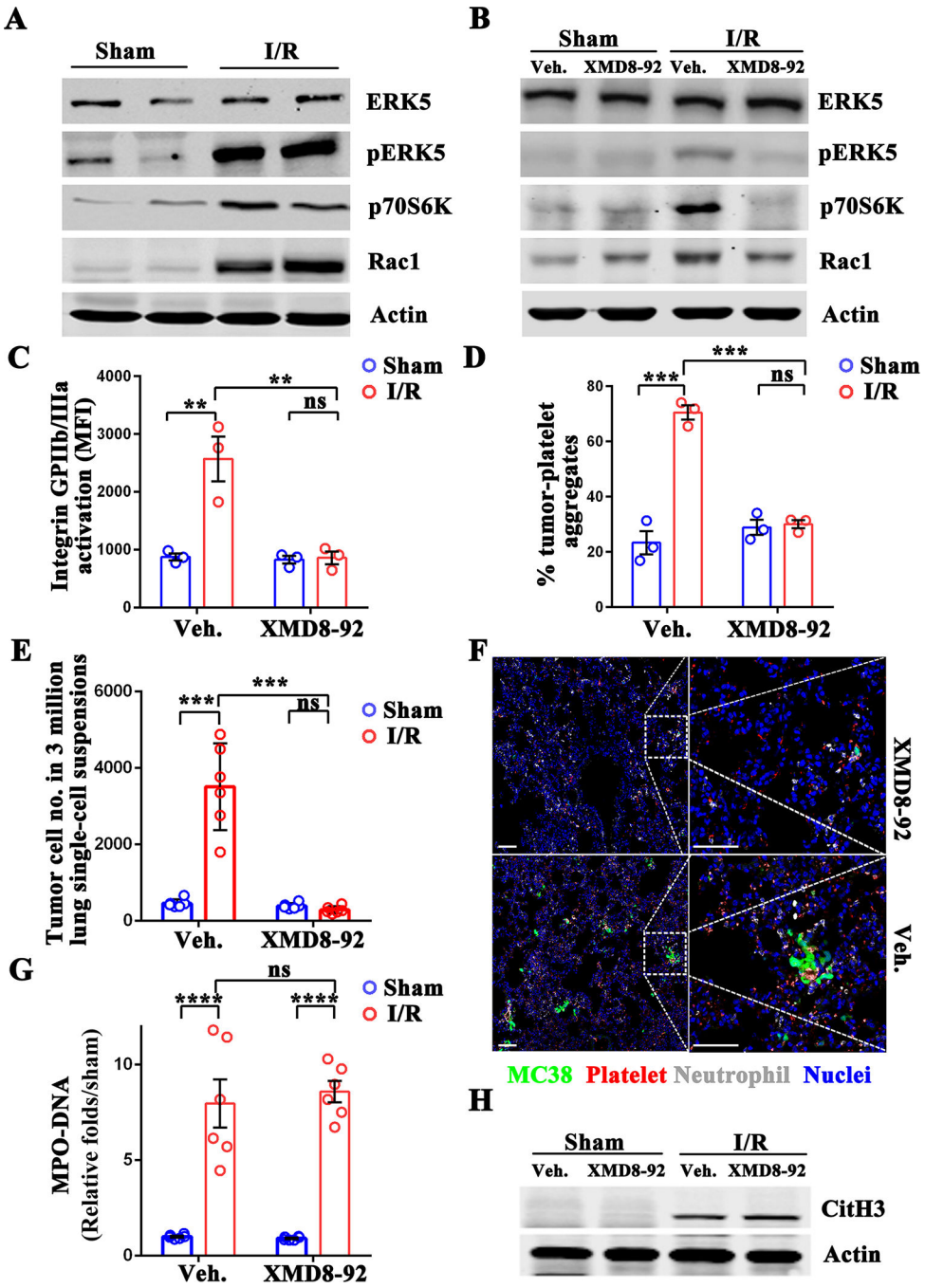

Figure 5.

Aggregation of platelets and CTCs under hepatic I/R stress is platelet ERK5-dependent. (A) Western blot analysis of ERK5, pERK5, p70S6K, and Rac1 proteins in platelets following 1.5 hours of hepatic ischemia and 3 hours of reperfusion. (B) Mice were given intraperitoneal injections of XMD8–92 (50 mg/kg) 6 hours prior to hepatic I/R. Protein levels in platelets 3 hours post I/R were determined by western blot. (C) Flow cytometric analysis of integrin activation in platelets extracted from XMD8–92 or vehicle-treated mice following sham laparotomy or hepatic I/R. (D) Aggregation capacity of platelets from C

with MC38 cells. (E) FACS quantitative data of MC38 cell numbers in the lungs of XMD8–92 or vehicle-treated mice 12 hours after tumor cell injection. (F) Representative immunofluorescence images showing tumor cells arrested at 24 hours following hepatic I/R in XMD8–92 or vehicle-treated mice. Green: MC-38; Red: Platelet; Grey: Neutrophil; Blue: Nuclei. Scale bar, 100μm. (G) Serum MPO-DNA complex levels were assessed in XMD8–92 or vehicle-treated mice following sham laparotomy or 1.5 hours of ischemia and 6 hours of reperfusion. (H) The level of Cit-H3 protein was determined by western blot analysis in XMD8–92 or vehicle-treated mice in G. Data are presented as mean ± SEM from n = 3–6 mice per group. ns: not significant, ** $P<0.01$, *** $P<0.001$ and **** $P<0.0001$.

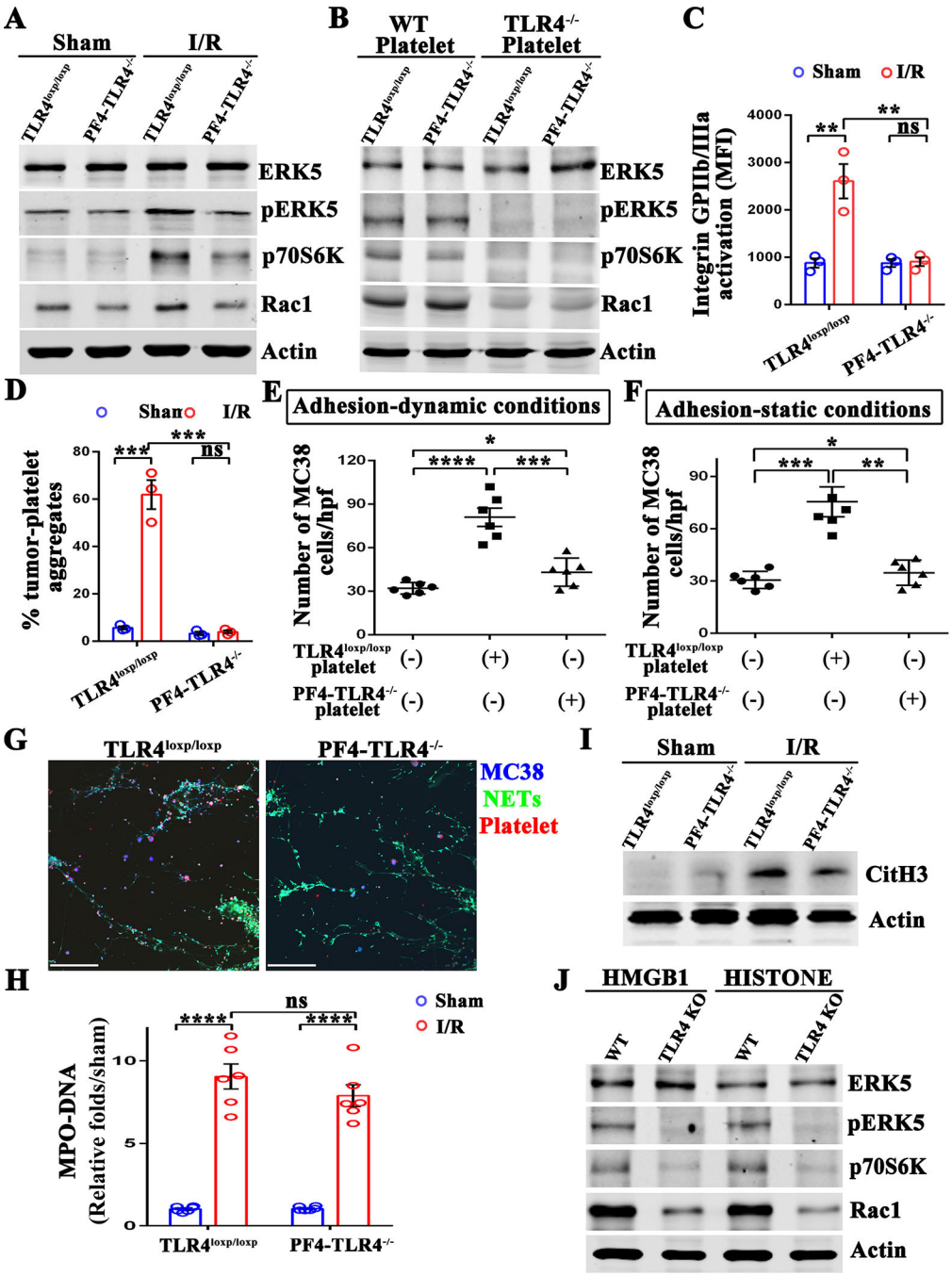

Figure 6.

Platelet TLR4 is essential for activation of ERK4 and NET-mediated capturing of tumor cells. (A) Western blot analysis of indicated proteins in the platelets extracted from TLR4 flox ($TLR4^{loxp/loxp}$) and platelet-specific TLR4-KO ($PF4\text{-}TLR4^{-/-}$) mice after either sham laparotomy or 1.5 hours of hepatic ischemia and 3 hours of reperfusion. (B) Platelets obtained from wild type and $TLR4^{-/-}$ mice were adoptively transferred into platelets-depleted $TLR4^{loxp/loxp}$ and $PF4\text{-}TLR4^{-/-}$ mice. Western blot analysis of indicated proteins in the platelets extracted from the above mice after 1.5 hours of hepatic ischemia and 3 hours

of reperfusion. (C) Flow cytometry analysis of integrin activation in platelets extracted from $TLR4^{loxp/loxp}$ and PF4-$TLR4^{-/-}$ mice after either sham laparotomy or hepatic I/R. (D) Aggregation capacity of platelets from C with MC38. (E and F) Quantitation of tumor cells that adhered to NETs in the presence of $TLR4^{loxp/loxp}$ or PF4-$TLR4^{-/-}$ platelets under static and dynamic conditions. (G) Representative immunofluorescent staining of tumor adhesion to NETs under static conditions. Blue: MC-38; Green: NETs; Red: Platelet. Scale bar, 100μm. (H) Serum MPO-DNA complex levels were assessed in $TLR4^{loxp/loxp}$ and PF4-$TLR4^{-/-}$ mice after either sham laparotomy or 1.5 hours of hepatic ischemia and 6 hours of reperfusion. (I) Western blot analysis of Cit-H3 protein level in mice from H. (J) Platelets isolated from wild type and $TLR4^{-/-}$ mice were stimulated with recombinant HMGB1 (5ug/ml) or histone protein (25ug/ml) for 6 hours. Western blot analysis of indicated proteins in these platelets. Data are presented as mean ± SEM from n = 3–6 mice per group. ns: not significant, *P<0.05, **P<0.01, ***P<0.001 and ****P<0.0001.

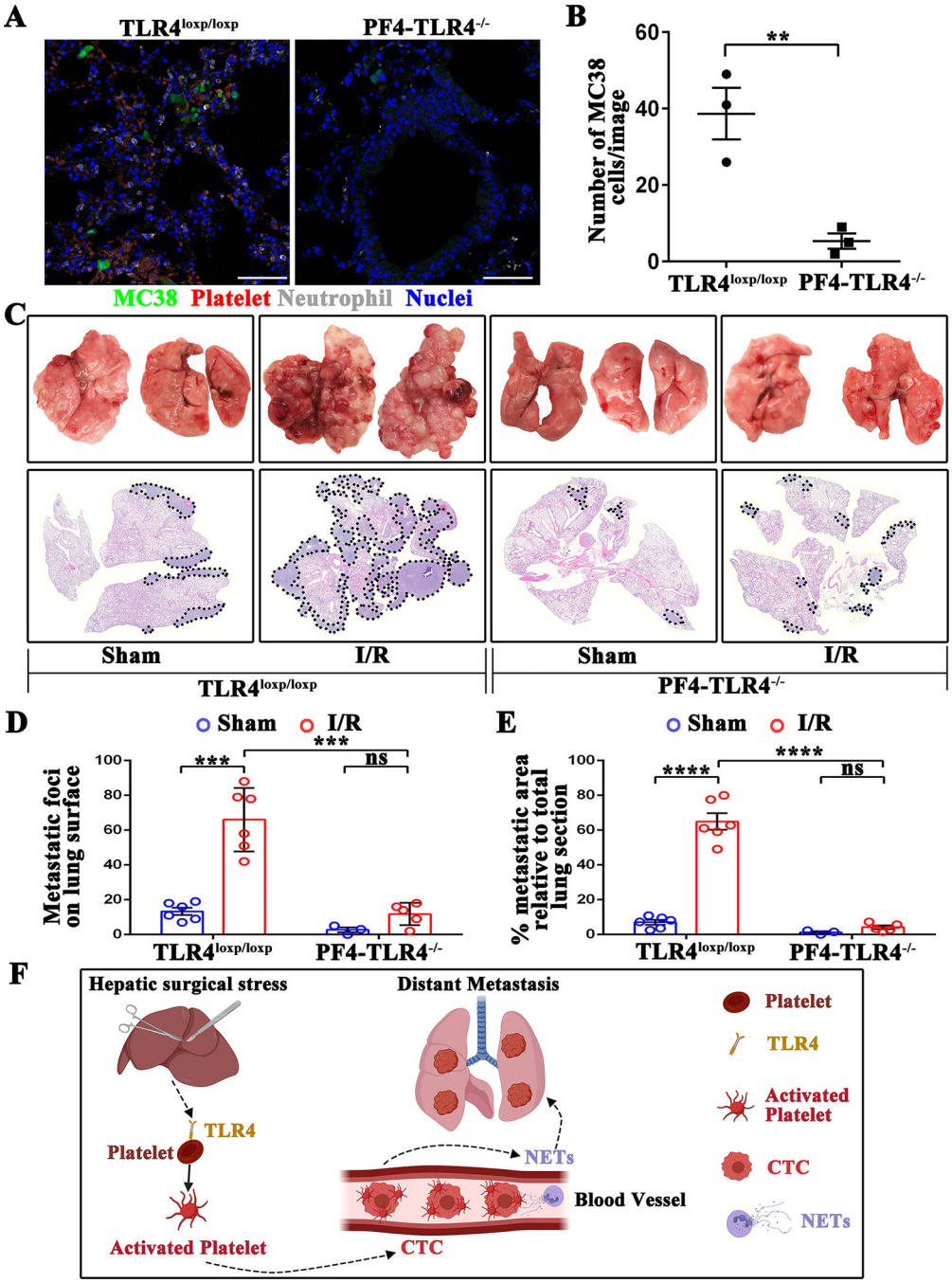

Figure 7.

Platelets-specific TLR4-KO significantly reduces surgical stress-induced metastasis *in vivo*. (A) Representative immunofluorescence images of confocal microscopy showing tumor cells in the lungs of TLR4$^{loxp/loxp}$ and PF4-TLR4$^{-/-}$ mice at 24 hours following hepatic I/R. Green: MC38; Red: Platelets; Gray: Neutrophil; Blue: Nuclei. Scale bar, 100μm. (B) Quantitation of individual tumor cells in the lungs of TLR4$^{loxp/loxp}$ and PF4-TLR4$^{-/-}$ mice at 24 hours following hepatic I/R. Points represent the mean ± SEM (n ≥ 9 images). (C) Representative images of pulmonary nodules and H&E staining of lung sections after

necropsy in TLR4$^{loxp/loxp}$ and PF4-TLR4$^{-/-}$ mice subjected to sham or I/R. (D) Tumor burden as determined by the number of metastatic pulmonary nodules 21 days after tumor cell injection in TLR4$^{loxp/loxp}$ and PF4-TLR4$^{-/-}$ mice subjected to sham or hepatic I/R group. (E) Tumor burden determined in mice from E as a percentage of lung replacement by metastatic tumors. Data are presented as mean ± SEM from n = 3–6 mice per group. ns: not significant, ** P<0.01, *** P<0.001 and **** P<0.0001. (F) Schematic diagram of the signaling pathways involved in hepatic I/R induced distant metastasis. Systematic expression of HMGB1 and histone after hepatic I/R activate platelet through TLR4-ERK5-integrin axis, which promotes platelet-tumor cell aggregate formation. Such aggregation facilitates the NET-mediated capture of platelet-tumor cell aggregates and then stimulate tumor cells migration, which promote subsequent tumor distant metastasis.